A Study on Auxiliary Circuit for Floating Bidirectional Power Flow Controller based on Partial Power Conversion

Yohei Sasaki [1] **Kenji Natori** [1] **Yukihiko Sato** [1]

1) Chiba University, Graduate School of Engineering, Chiba, Japan

E-mail: knatori@chiba-u.jp

ABSTRACT: This paper studies an auxiliary circuit for a floating bidirectional power flow controller (F-BPFC) that has been proposed based on partial power conversion (PPC) principle. As the auxiliary circuit, a circuit that enables bidirectional power supplies i.e. powering F-BPFC and regeneration from F-BPFC is required. In this paper, we study a CLLC resonant converter that achieves bidirectional and high-efficiency power supply by accomplishing zero-voltage switching (ZVS) and zero-current switching (ZCS). Effectiveness of the adoption of the CLLC resonant converter as the auxiliary circuit is verified by experimental results.

KEY WORDS: floating bidirectional power flow controller (F-BPFC), partial power conversion (PPC), auxiliary circuit, CLLC resonant converter

1. INTRODUCTION

In recent years, DC microgrid that actively integrates renewable energy sources has been drawing much attention as a promising candidate to overcome environmental issues like global warming [(1)-(3)]. Since many renewable energy sources and energy storage devices have DC input and output terminals, DC microgrid achieves high-efficiency power systems by reducing power conversions between DC and AC. To accomplish stable DC microgrid or stable connection of DC microgrids, power flow controllers that control power flows among the nodes are required.

Our research group has been studying the power flow controllers and the control methods and has proposed a bidirectional power flow controller (BPFC) [(4)] and a floating bidirectional power flow controller (F-BPFC) [(5)]. Furthermore, we have studied the extensions of the BPFC and the F-BPFC to multi-terminal cases [(6), (7)]. F-BPFC is a modified version of BPFC and achieves high-efficiency power flow control by floating the main circuit. In the main circuit of F-BPFC, only the minimum power that is necessary for the power flow control is used for controlling the power flow. Therefore, it achieves high-efficiency power flow control. The concept is based on partial power conversion (PPC) principle [(8)-(10)].

Fig. 1 shows a schematic of the PPC. In the case of general power conversion, majority of the rated power is converted at the circuit. On the other hand, in the case of PPC, majority of the rated power is not converted and only small part of the rated power that is necessary for controlling the power flow is converted at the circuit. Therefore, the PPC significantly reduces the losses generated in the conversion and achieves high-efficiency power conversion.

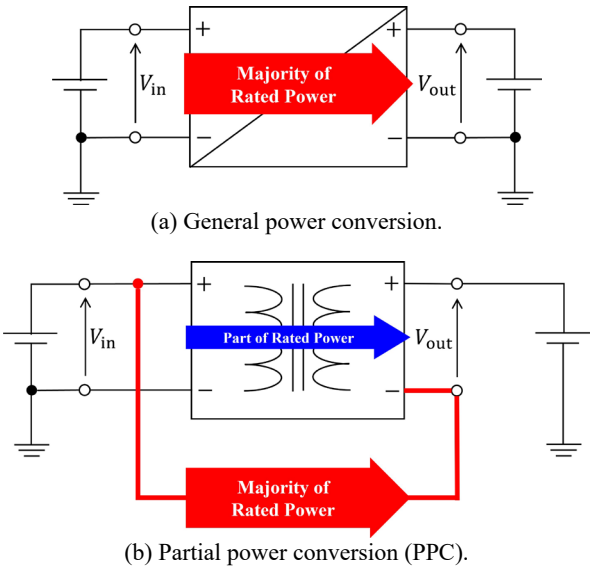

Fig. 1 Comparison of power conversion methods.

The power flow control system by using F-BPFC consists of the floated main circuit (F-BPFC) and an auxiliary circuit that enables bidirectional power supplies (powering F-BPFC and regeneration from F-BPFC) as shown in Fig. 2. However, the auxiliary circuit has not been studied in detail, since the power converted at the auxiliary circuit is slight compared to the main circuit.

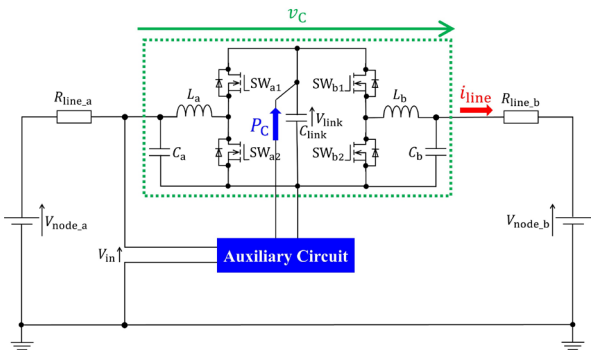

Fig. 2 Circuit diagram of power flow control system by using F-BPFC.

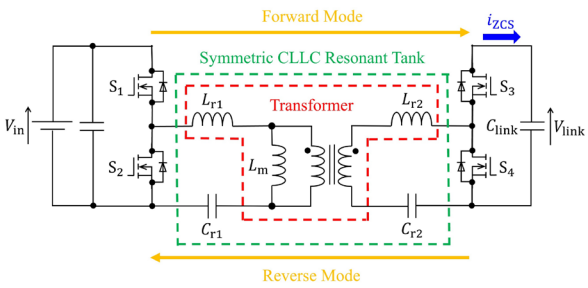

Fig. 3 Circuit diagram of CLLC resonant converter.

In this paper, we study the auxiliary circuit that achieves bidirectional power supplies. As the topology, we adopt a CLLC resonant converter that achieves ZVS and ZCS. Then, by using the CLLC resonant converter as the auxiliary circuit, high-efficiency power flow control system with F-BPFC is realized.

2. OPERATION PRINCIPLE OF F-BPFC

Fig. 2 shows a circuit configuration of the F-BPFC. By using the F-BPFC, the voltage $v_C = (D_b - D_a)V_{link}$ is generated between the two nodes (D_a and D_b are duty ratios of the switches SW_{a1} and SW_{b1}). Then, the current i_{line} is given as follows:

$$i_{line} = \frac{v_C + V_{node\_a} - V_{node\_b}}{R_{line\_a} + R_{line\_b}}. \quad (1)$$

In the case of $V_{node\_a} = V_{node\_b}$, the current is described as follows:

$$i_{line} = \frac{v_C}{R_{line\_a} + R_{line\_b}} = \frac{(D_b - D_a)V_{link}}{R_{line\_a} + R_{line\_b}}. \quad (2)$$

Therefore, the power flow is controlled by D_a and D_b. Note that the node voltages are not converted to control the power flow, and only the link capacitor voltage V_{link} is converted to control the power flow. Generally, V_{link} is significantly smaller than the node voltages, the power flow control is achieved with very small losses. In other words, only the required small power is used to control the power flow. This is the concept of PPC. Here, the consumed power at the F-BPFC is as below.

$$P_C = v_C i_{line} = (R_{line\_a} + R_{line\_b}) i_{line}^2 \quad (3)$$

The equation means that the consumed power at the F-BPFC is equal to the loss at the line resistances. The consumed power is provided from the link capacitor C_{link} and the voltage V_{link} will decrease as the consumed power increases. Therefore, the auxiliary circuit that supplies power to the link capacitor C_{link} shown in Fig. 2 is required to keep the voltage of C_{link}.

In the case of $V_{node\_a} \neq V_{node\_b}$, i_{line} is given as (1). Then, the consumed power at the F-BPFC is as follows:

$$P_C = v_C i_{line} = (R_{line\_a} + R_{line\_b}) i_{line}^2 - (V_{node\_a} - V_{node\_b}) i_{line}. \quad (4)$$

It means that there is a possibility that $P_C < 0$ when $V_{node\_a} > V_{node\_b}$. In such cases, the link capacitor voltage of V_{link} increases. Therefore, the auxiliary circuit is required to supply power from the link capacitor C_{link} to the node A to keep the voltage of C_{link}. That is the reason why the auxiliary circuit need to have ability to achieve bidirectional power supplies.

3. AUXILIARY CIRCUIT

In this section, we introduce the auxiliary circuit. First, the functions that are required for the auxiliary circuit are described and the CLLC resonant circuit is selected as the topology of the auxiliary circuit. Then, control modes of the CLLC resonant circuit are introduced. Finally, the dead-band control of the CLLC resonant circuit is presented.

3. 1. Circuit Topology

As previously introduced, the auxiliary circuit is required to have the ability of bidirectional power supplies (powering F-BPFC and regeneration from F-BPFC). In addition, it is required to be isolated. Here, since the difference of the voltage between V_{node_a} and V_{link} is large (F-BPFC is based on PPC), the turns ratio of the transformer is large. Therefore, the leakage inductance should be effectively used in the auxiliary circuit. Considering the conditions above, this paper adopts the CLLC resonant circuit shown in Fig. 3 as the auxiliary circuit. An example of the operation waveforms is shown in Fig. 4. It is expected that it achieves zero voltage switching (ZVS) at the primary side and zero current switching

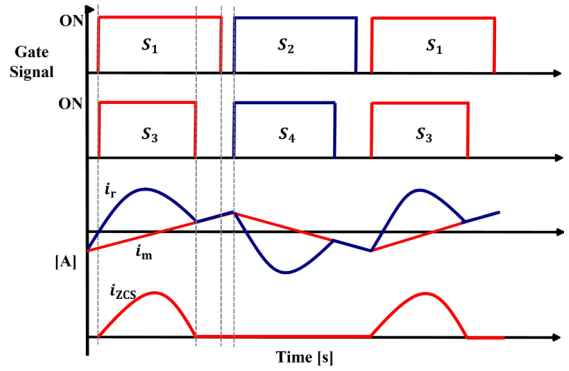

Fig. 4 Operation waveforms of CLLC resonant converter.

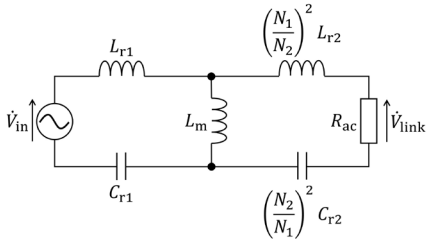

Fig. 5 Equivalent circuit seen from the primary side of CLLC resonant converter.

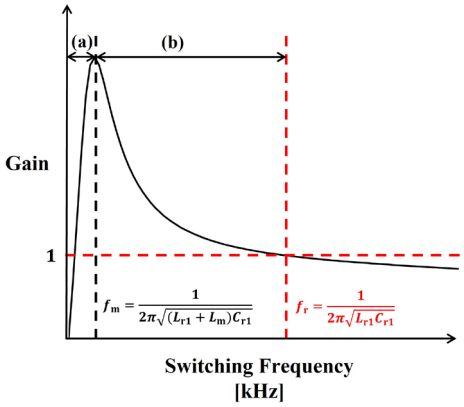

Fig. 6 Input to output frequency characteristics of CLLC resonant converter.

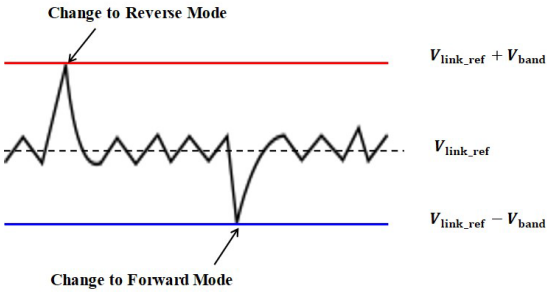

Fig. 7 Schematic of dead-band control.

(ZCS) at the secondary side. Consequently, the CLLC resonant converter is expected to accomplish high-efficiency bidirectional power supply.

3. 2. Control Modes

The equivalently converted circuit of Fig. 3 seen from the primary side is depicted as Fig. 5. From Fig. 5, the voltage ratio between the input and the output is derived as follows:

$$\frac{|\dot{V}_{link}|}{|\dot{V}_{in}|} = \frac{1}{\sqrt{\left(1+\frac{1}{S}-\frac{1}{SF^2}\right)^2+\left(F-\frac{1}{F}\right)^2\left(\frac{Q_1}{N^2}+Q_2\left(1+\frac{1}{S}-\frac{1}{SF^2}\right)\right)^2}} \quad (5)$$

where $N = \frac{N_1}{N_2}$, $S = \frac{L_m}{L_{r1}}$, $F = \frac{f_{SW}}{f_r}$, $Q_1 = \frac{1}{R_{ac}}\sqrt{\frac{L_{r1}}{C_{r1}}}$, $Q_2 = \frac{1}{R_{ac}}\sqrt{\frac{L_{r2}}{C_{r2}}}$.

Then, the frequency characteristics are given as shown in Fig. 6. Fig. 6 demonstrates that the voltage ratio decreases as the switching frequency increases in the region (b). It means it is possible to control the output voltage of the CLLC resonant circuit by changing the frequency. Therefore, the circuit enables to achieve bidirectional and high-efficiency power supply.

3. 3. Dead-Band Control

At the rectification side, introduction of a synchronous rectification achieves higher-efficiency power supply and seamless change of the direction. However, in the case of light-load operation, the efficiency significantly deteriorates when the synchronous rectification is adopted. Therefore, diode rectification should be used in the case of light-load operation to prevent the efficiency degradation. Here, when using diode rectification, it is impossible to seamlessly change the direction of the power supply. For example, when the switches S_3, S_4 in Fig. 3 are off and those are used as the diode rectification mode, the power supply direction is from the primary side to the secondary side. On the other hand, the switches S_1, S_2 in Fig. 3 are off and those are used as the diode rectification mode, the power supply direction is from the secondary side to the primary side.

Then, in addition to the voltage control by the frequency change, we introduce a dead-band control [11] as a mean for changing the power supply direction. The schematic of the dead-band control is shown in Fig. 7. When the link voltage V_{link} becomes larger than the upper threshold, the mode is switched from the forward direction (powering) mode to the reverse direction (regeneration) mode. On the other hand, the link voltage V_{link} is lower than the

Table 1 Parameters of F-BPFC.

Switching Frequency	f_{SW}	10 kHz
Node Voltage	V_{node}	$48-53$ V
Link Voltage	V_{link}	10 V
Capacitance	$C_a, C_b/C_{link}$	100 μF / 47 μF
Inductance	L_a, L_b	0.6 mH

Table 2 Parameters of auxiliary circuit (CLLC resonant converter).

Resonant Frequency	f_r	30 kHz
Magnetization Inductance	L_m	265 μH
Leakage Inductance	L_{r1}/L_{r2}	17.8 μH/1.205 μH
Resonant Capacitance	C_{r1}/C_{r2}	1.58 μF/35 μF

lower threshold, the operation mode is changed from the reverse direction (regeneration) mode to the forward direction (powering) mode. The link voltage V_{link} is controlled by the dead-band control in this way.

4. EXPERIMENT

This section presents experimental evaluation of the effectiveness of the auxiliary circuit. Parameters of the main circuit (F-BPFC) are summarized in Table 1 and those of the CLLC resonant circuit as the auxiliary circuit are shown in Table 2. In the experiment, the turns ratio of the transformer is set as $N_1 : N_2 = 30 : 6$.

Experimental results of the two modes (shown in Fig. 3) described below are studied in the following subsections.

[Forward Mode] Auxiliary circuit supplies the power from the node A to the F-BPFC (powering) since the grid voltages are set as $V_{node\_A} = V_{node\_B} = 50$[V].

[Reverse Mode] Auxiliary circuit supplies the power from the F-BPFC to the node A (regeneration) since the grid voltages are set as $V_{node\_A} = 52$ V, $V_{node\_B} = 48$ V.

4. 1. Waveform of Auxiliary Circuit

The experimental results when the power flow is controlled to be 140 W from the node A to the node B are shown in Figs. 8 (a) [Forward Mode] and 8 (b) [Reverse Mode]. In both results, i_{line} is the current that flows from the node A to the node B (shown in Fig. 2) and i_{ZCS} is the current flowing from the node A to the link capacitor C_{link} of the F-BPFC (shown in Fig. 3). It is confirmed

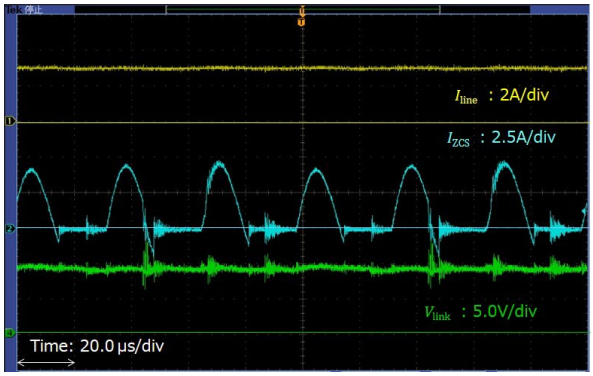

(a) [Forward Mode]

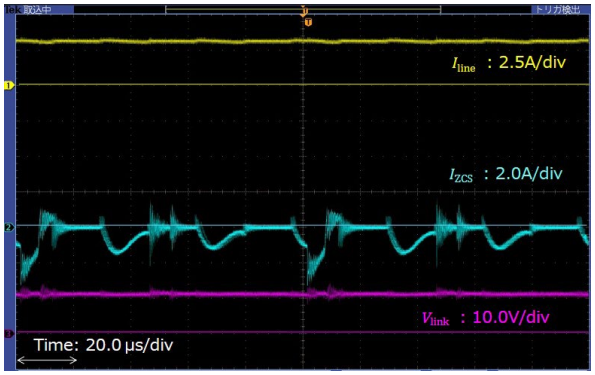

(b) [Reverse Mode]

Fig. 8 Waveforms of experiment.

that i_{line} is controlled as the required value and the power flow control is achieved in both modes. In the case of [Forward Mode] (Fig. 8 (a)), i_{ZCS} is positive value and it means that the auxiliary circuit supplies the power from the node A to the F-BPFC. It seems that the ZCS is partly achieved. However, due to the oscillation, ZCS seems to be failed sometimes. On the other hand, in the case of [Reverse Mode] (Fig. 8 (b)), the current flows from the F-BPFC to the node A, since i_{ZCS} is negative value. It seems that the ZCS is sometimes accomplished, but it is failed in most cases because of the serious oscillations. Consequently, it leads to the efficiency deterioration.

The oscillation (ringing) is supposed to be caused by the parasitic inductance of the wire and the output capacitance of the power switching device of the F-BPFC as shown in Fig. 9. It is induced by the hard switching of the power switching devices of the F-BPFC. To reduce the oscillation, there are several approaches (modification of the circuit board to shorten the wires, use of the power switching devices with small output capacitance, and so on). We changed the power switching device from the one of 2000 pF output capacitance to another of 400 pF output capacitance at $V_{DS} = 10V$ to improve the oscillation. Fig. 10

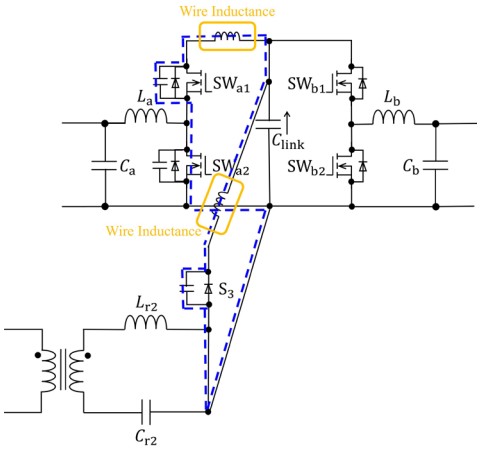

Fig. 9 Schematic of oscillation (ringing) generation.

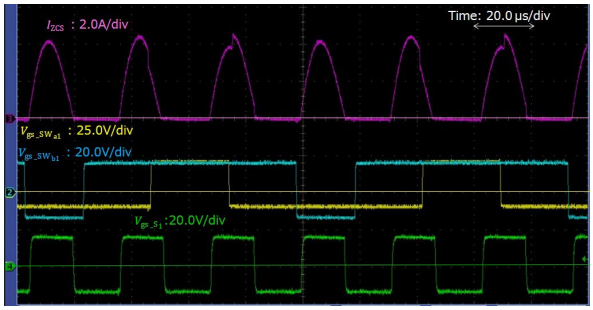

Fig. 10 Waveforms after change of power switching device [Forward Mode].

shows the experimental waveforms in the case of [Forward Mode] after the change of the power switching device. It is confirmed that the oscillations of i_{ZCS} are significantly reduced, and ZCS is successfully achieved.

4. 2. Efficiency Measurement

Efficiency measurement results of the F-BPFC and the auxiliary circuit (whole system) are shown in Fig. 11 and those of only the auxiliary circuit are shown in Fig. 12. The results in the case of [Forward Mode] are shown in Figs. 11 (a) and 12 (a), and the results in the case of [Reverse Mode] are shown in Figs. 11 (b) and 12 (b).

Fig. 11 demonstrates that the F-BPFC and the auxiliary circuit (whole system) achieves high-efficiency power flow control regardless of the operation modes of the auxiliary circuit.

In Fig. 12, the efficiency measurement results of only the auxiliary circuit are shown. Fig. 12 (a) shows the results in the case of [Forward Mode] and the green dots show the results of a commercial isolated unidirectional converter (TRACOPOWER TEN40-7213WIR) for comparison. It is confirmed that the efficiency of the studied auxiliary circuit is higher than that of the commercial one. The efficiency is improved by achievement of ZVS and ZCS. In the case of [Reverse Mode], when the power flow between the node A and the node B becomes large, the auxiliary circuit becomes light-load operation (refer to (4)). Therefore, at the range of large power flow in Fig. 12 (b), the efficiency in the case of the synchronous rectification is worse than that in the case of the diode rectification. It is confirmed that the diode rectification achieves higher efficiency in the region of light-load operation.

5. CONCLUSION

In this paper, we studied the auxiliary circuit for the F-BPFC. As the auxiliary circuit that is isolated and enables bidirectional power supplies, the CLLC resonance converter was adopted. The experimental results demonstrated that the auxiliary circuit achieved high-efficiency bidirectional power supplies by realizing ZVS and ZCS.

REFERENCES

(1) T. Dragičević, X. Lu, J. C. Vasquez and J. M. Guerrero, "DC Microgrids—Part I: A Review of Control Strategies and Stabilization Techniques," in *IEEE Transactions on Power Electronics*, vol. 31, no. 7, pp. 4876-4891, July 2016.

(2) T. Dragičević, X. Lu, J. C. Vasquez and J. M. Guerrero, "DC Microgrids—Part II: A Review of Power Architectures, Applications, and Standardization Issues," in *IEEE Transactions on Power Electronics*, vol. 31, no. 5, pp. 3528-3549, May 2016.

(3) L. Tang and B. -T. Ooi, "Locating and Isolating DC Faults in Multi-Terminal DC Systems," in *IEEE Transactions on Power Delivery*, vol. 22, no. 3, pp. 1877-1884, July 2007.

(4) K. Natori, H. Obara, K. Yoshikawa, B. C. Hiu and Y. Sato, "Flexible power flow control for next-generation multi-terminal DC power network," *2014 IEEE Energy Conversion Congress and Exposition (ECCE)*, 2014.

(5) T. Tanaka, Y. Takahashi, K.Natori, and Y. Sato, "High-Efficiency Floating Bidirectional Power Flow Controller for Next-Generation DC Power Network," *IEEJ Journal of Industry Applications*, vol. 7, no. 1, pp. 29-34, 2018.

(6) Y. Takahashi, K. Natori, and Y. Sato, "A multi-terminal power flow control method for next-generation DC power network," *2015 IEEE Energy Conversion Congress and Exposition (ECCE)*, Montreal, QC, Canada, 2015.

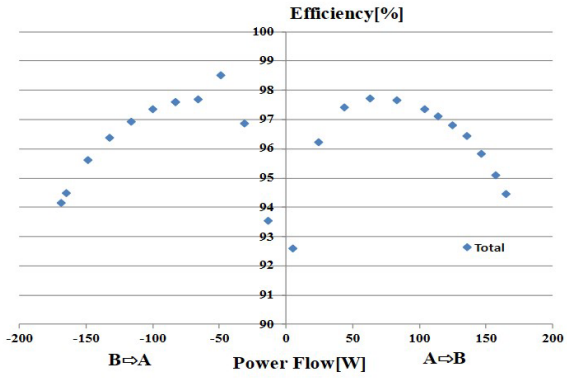

(a) [Forward Mode]

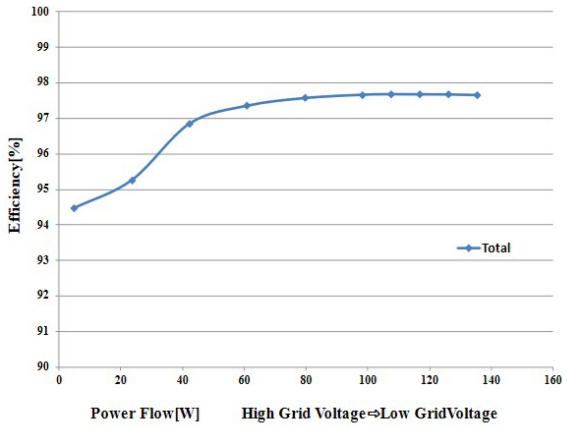

(b) [Reverse Mode]

Fig. 11 Efficiency of F-BPFC and auxiliary circuit (whole system).

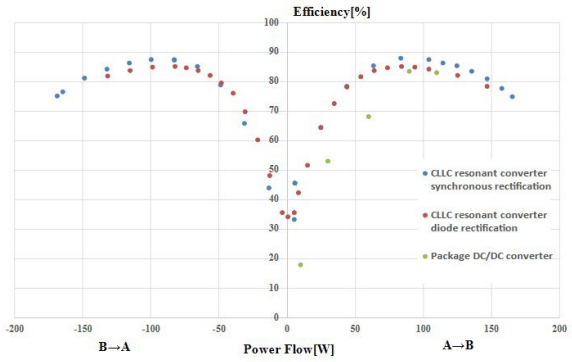

(a) [Forward Mode]

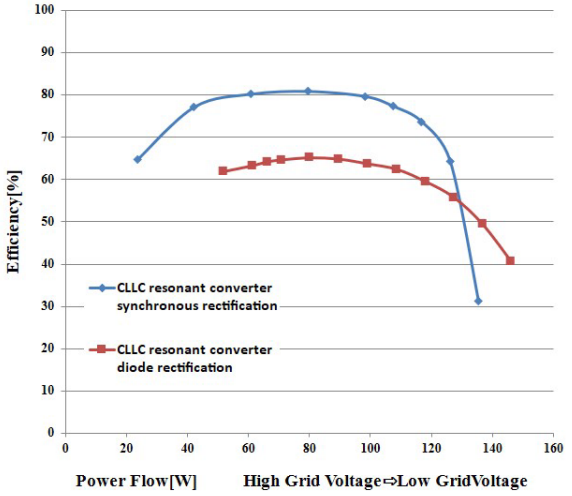

(b) [Reverse Mode]

Fig. 12 Efficiency of only auxiliary circuit.

(7) K. Natori, T. Tanaka, Y. Takahashi, and Y. Sato, "A study on high-efficiency floating multi-terminal power flow controller for next-generation DC power networks," 2017 *IEEE Energy Conversion Congress and Exposition (ECCE)*, 2017.

(8) J. Zhao, K. Yeates and Y. Han, "Analysis of high efficiency DC/DC converter processing partial input/output power," *2013 IEEE 14th Workshop on Control and Modeling for Power Electronics (COMPEL)*, 2013.

(9) M. W. Ahmad and S. Anand, "Power decoupling in solar PV system using partial power processing converter," *2016 10th International Conference on Compatibility, Power Electronics and Power Engineering (CPE-POWERENG)*, 2016.

(10) J. R. R. Zientarski, M. L. da Silva Martins, J. R. Pinheiro and H. L. Hey, "Evaluation of Power Processing in Series-Connected Partial-Power Converters," in *IEEE Journal of Emerging and Selected Topics in Power Electronics*, vol. 7, no. 1, pp. 343-352, March 2019.

(11) M. -H. Ryu, H. -S. Kim, J. -W. Baek, H. -G. Kim and J. -H. Jung, "Effective Test Bed of 380-V DC Distribution System Using Isolated Power Converters," in *IEEE Transactions on Industrial Electronics*, vol. 62, no. 7, pp. 4525-4536, July 2015.